

**IMECE 2007- 41295**

**EXPERIMENTAL MEASUREMENTS AND NUMERICAL MODELING VALIDATION OF  
TEMPERATURE DISTRIBUTION IN TISSUE MEDIUM DURING SHORT PULSE  
LASER IRRADIATION**

**Ashim Dutta<sup>1</sup>**

**Kyunghan Kim<sup>2</sup>**

**Kunal Mitra<sup>1</sup>**

**Zhixiong Guo<sup>2</sup>**

**<sup>1</sup> Mechanical and Aerospace Engineering Department  
Florida Institute of Technology  
Melbourne, FL 32901**

**<sup>2</sup> Department of Mechanical and Aerospace Engineering  
Rutgers, The State University of New Jersey  
Piscataway, NJ 08854**

**ABSTRACT**

The objective of this paper is to analyze the temperature distributions and heat affected zone in skin tissue medium when irradiated with either a collimated or a focused laser beam from a short pulse laser source. Single-layer and three-layer tissue phantoms containing embedded inhomogeneities are used as a model of human skin tissue having subsurface tumor. Q-switched Nd:YAG laser is used in this study. Experimental measurements of axial and radial temperature distribution in the tissue phantom are compared with the numerical modeling results. For numerical modeling, the transient radiative transport equation is first solved using discrete ordinates method for obtaining the intensity distribution and radiative heat flux inside the tissue medium. Then the temperature distribution is obtained by coupling the bio-heat transfer equation with either hyperbolic non-Fourier or parabolic Fourier heat conduction model. The hyperbolic heat conduction equation is solved using MacCormack's scheme with error terms correction. It is observed that experimentally measured temperature distribution is in good agreement with that predicted by hyperbolic heat conduction model. The experimental measurements also demonstrate that converging laser beam focused directly at the subsurface location can produce desired high temperature at that location as compared to that produced by collimated laser beam for the same laser parameters.

**INTRODUCTION**

Over the last few years, lasers have successfully been used for various thermal therapy of tumors for applications like Laser Induced Hyperthermia [1], Laser Interstitial

Thermotherapy (LITT) of mammary tumors [2], and deep tumor ablation [3]. Though majority of the tumor irradiation techniques use continuous wave (CW) or long pulsed laser, however, short pulsed lasers are recently being preferred for these applications [4]. The ability to produce highly localized heating at the desired location has made pulse laser attractive for tumor irradiation compared to the CW lasers. This is because for the same energy input, the instantaneous peak power attained during pulsed laser irradiation is greater than that obtained in CW laser irradiation [5].

It has been well established that the tissues are sensitive to the temperature rise. The thermal impact on tissue changes drastically when the temperature rise exceeds 43°C [3]. It has been found that peak temperature in the range of 60°C to 80°C is required to ensure complete tumor necrosis without any post-treatment trauma [6]. However, it has been also observed that temperature required to kill the tumor tissue depends on the exposure time [7, 8]. Robinson et al [9] has predicted that temperature elevation to at least 56°C for 1 second or more should be sufficient to kill cancer cells. Thus there is no general consensus in the literature about the exact extent of temperature rise and exposure time necessary for complete tumor ablation.

Adoption of proper beam delivery technique is very important to initiate photo-thermal or photo-ablative effect for complete destruction of tumor. Selection of proper beam delivery technique depends mainly on the location of the tumor in the body. If the tumors are located deep inside the body then fiber-optic delivery system is used to transport laser light to the tumor site [10, 11]. These fibers deliver the beam either in the form of collimated beam or in the form of diffused beam. Due to the collimated or diffused nature of the beam as used in

tumor irradiation therapies like Laser Induced Hyperthermia and LITT, high power and long exposure time is required to achieve the desired fluence. This often leads to significant heat spread damaging surrounding healthy tissues. Moreover, fibers are often inserted into the tumor site to achieve volumetric heating. Same technique of piercing of fiber into the tumor is also used for irradiating subsurface tumors. However, for skin tumors or subsurface tumors this perforation of the skin can be eliminated if a converging laser beam focused at the subsurface location is used. It has already been demonstrated that depending on the wavelength of irradiation, depth of penetration during laser-tissue interaction can reach as deep as 1 cm [12]. However, if collimated or diffused beam is used, most of the energy gets absorbed by tissue at the skin surface.

The technique of focusing laser beam at the treatment location using a converging lens can reduce the absorption of laser energy by the skin. Due to the concentration of energy in a focused beam, it can penetrate the skin and reach at greater depth without significant attenuation. Theoretical study has already been performed demonstrating this significant increase in peak absorption at the focal plane [13]. As a result of peak absorption at the focal plane, a desired subsurface temperature higher than the surface temperature can be achieved. This technique has been used for applications such as Non-ablative Dermal Remodeling [14, 15] and treatment of striated muscles [16]. In this paper, this technique of using converging laser beam focused at the subsurface tumor location is used to achieve desired temperature at the tumor tissue keeping the surface temperature under control.

A detailed understanding of bio-heat transfer phenomenon is required to design a new method which can ensure accurate and controlled deposition of energy into the exact location of biological tissues with minimum collateral thermal damage to adjoining healthy tissue during any laser therapy. Substantial efforts have been made previously to develop a complete theoretical model considering the inherent complexity of the heat transfer process in tissue medium. Traditional analysis of heat transfer by conduction in biological tissues is performed using Fourier's law. In Fourier's law, heat conduction is assumed to be an instantaneous process with an infinite speed of propagation of the thermal signal, indicating that a local thermal change causes an instantaneous perturbation in the temperature at the each point in the medium, even if the intervening distances are very large. To consider a finite speed of propagation, damped wave models have been proposed which lead to a hyperbolic heat conduction equation [17] or Dual Phase Lag (DPL) equation [18]. With the development of this damped wave model theory of heat diffusion, an important parameter called thermal relaxation time ( $\tau$ ) needs to be considered [18-21]. Thermal relaxation time is a material property which indicates the time required for the heat flux to adjust or relax to the changes in the temperature gradient. It has already been demonstrated that heat transfer processes which occur for time periods less than the relaxation time of the medium may yield incorrect results if the Fourier model is used for applications such as burning of skin subjected to instantaneous heating [22] and cryo-preservation of skin [23].

Comparison of results obtained from numerical modeling with the experimental measurements is of prime importance for designing efficient technique of thermal

irradiation of tumors. For the study of heat affected zone in skin tissue phantoms using collimated laser beam, experimental measurements have been compared with numerical modeling results obtained using one-dimensional Fourier heat conduction model [24] and two-dimensional axisymmetric hyperbolic heat conduction formulations [25]. Validity of the use of hyperbolic heat conduction formulation for the case of bologna meat samples when irradiated with a collimated laser beam from a short pulse or CW laser source has been also reported in the literature [25].

Most of the previous numerical works have modeled the laser source term in bio-heat transfer equation by either Lambert's law or diffusion approximation. The scattering effect is hardly incorporable in Lambert's law. The diffusion approximation is limited to predominant scattering medium. Such treatment can introduce significant error in temperature distribution in practical nonhomogeneous tissue medium [26] during short pulse laser irradiation, in which case light suffers significant scattering in most region and strong localized absorption in the target spot. Therefore, it is necessary to consider complete light transport through the tissue medium for analyzing bio-heat transport in tissues during short pulse laser irradiation.

No study has been reported in the literature which uses focused laser beam from a short pulse laser source for irradiation of subsurface tumors. The current work focuses on analyzing experimentally and numerically axial and radial temperature distribution in single-layer phantoms and multi-layer tissue phantoms simulating skin and containing inhomogeneity simulating tumor. For multi-layer skin tissue phantom each layer has different optical properties. The phantoms are irradiated by a Q-switched Nd:YAG short pulse laser source which is focused directly at the inhomogeneity location using a converging lens. The effectiveness of using a focused beam rather than a collimated beam to obtain the required temperature rise at the region of interest with smaller heat affected zone is demonstrated. The experimental results are compared with the numerical results obtained using Pennes' bio-heat transfer equation coupled with either Fourier parabolic or non-Fourier hyperbolic heat conduction model. Results of multi-layer tissue phantoms are also compared with those of single-layer tissue phantom.

## NOMENCLATURE

$c$	speed of light
$C_p$	specific heat of tissue
$R_D$	beam radius at the focal plane
$R_o$	beam radius at the sample surface
$T$	temperature
$k_a$	absorption coefficient of tissue
$k_e$	extinction coefficient
$k_s$	scattering coefficient of tissue
$q$	heat flux
$r, z$	spatial coordinates
$t$	time
$t_p$	pulse width of laser beam
$u(t)$	unit step function
$\alpha$	thermal diffusivity of tissue
$\delta(t)$	Dirac delta function
$\kappa$	thermal conductivity of tissue

$\mu, \eta, \xi$	direction cosines
$\rho$	density of tissue
$\tau$	relaxation time
$\Phi$	phase function
$\Omega$	solid angle

## MATHEMATICAL FORMULATION

The intensity redistribution inside the tissue medium as shown in Fig. 1 due to scattering of light in the tissue medium is obtained by solving the transient radiative transport equation [27, 28]:

$$\frac{1}{c} \frac{\partial I(r, z, \Omega, t)}{\partial t} + \frac{\mu}{r} \frac{\partial}{\partial r} [rI] - \frac{1}{r} \frac{\partial}{\partial \phi} [\eta I] + \xi \frac{\partial I}{\partial z} + k_e I = \frac{k_s}{4\pi} \int_{4\pi} \Phi(\Omega', \Omega) I(r, z, \Omega', t) d\Omega + S(r, z, \Omega, t) \quad (1)$$

where  $I$  is the scattered diffuse intensity,  $k_e$  and  $k_s$  are the extinction coefficient and the scattering coefficient respectively,  $\phi$  is the azimuthal angle,  $\Phi$  is the phase function,  $\Omega$  is the solid angle,  $c$  is the velocity of light in the medium,  $r$  and  $z$  are the spatial coordinates,  $t$  is the time, and  $S$  is the source term due from laser irradiation.

To calculate the source term  $S$  the laser beam is assumed to be Gaussian in both spatial and temporal domain and it is expressed as follows:

$$S(r, z, \Omega, t) = \frac{k_s}{4\pi} I_c (\mu^c \mu + \eta^c \eta + \xi^c \xi) \quad (2)$$

where the unit vector of  $(\mu^c, \eta^c, \xi^c)$  represents the collimated laser incident direction. The collimated intensity  $I_c$  is given by:

$$I_c(r, z, t) = L_0 \exp \left\{ -4 \ln 2 \times [(t - z/c) / t_p - 1.5]^2 \right\} \times \exp(-2r^2 / \sigma(z)^2) \times \exp(-k_e z) \quad (3)$$

where  $L_0$  is the maximum intensity of the laser beam at the sample surface,  $t_p$  is the laser pulse width, and  $\sigma(z)$  is the beam radius which the peak intensity drops to the  $e^{-2}$  value.

In the case of a converging laser beam as used in this paper which is focused at a depth of  $z = f_D$ , the standard deviation  $\sigma(z)$  in Eq. (3) varies with  $z$  and can be expressed as follows:

$$\sigma(z) = \sigma(0) \left( \frac{-(R_0 - R_D)}{R_0} \frac{z}{f_D} + 1 \right) \quad , \quad 0 \leq z \leq f_D \quad (4)$$

$$\sigma(z) = \sigma(0) \left( \frac{(R_0 - R_D)}{R_0} \frac{z}{f_D} - \frac{(R_0 - 2R_D)}{R_0} \right) \quad , \quad z > f_D$$

where  $\sigma(0)$  is the standard deviation of radial intensity distribution at the sample surface,  $R_0$  is the beam radius at the surface of the sample and  $R_D$  is radius of the beam at the focal plane.

Once the intensity distribution within the tissue medium is obtained, the corresponding temperature distribution is calculated by numerically solving Pennes' energy equation coupled with proper heat conduction model. In this paper both Fourier parabolic heat and non-Fourier hyperbolic heat conduction model is considered.

Pennes' energy equation for a tissue medium has the following form:

$$-\nabla \cdot q(r, z, t) - \omega \rho_b C_b T(r, z, t) - \nabla \cdot q^r(r, z, t) = \rho C_p \frac{\partial T(r, z, t)}{\partial t} \quad (5)$$

where  $\rho$  is the density of tissue,  $\rho_b$  is the density of blood,  $\omega_b$  is blood perfusion rate,  $C_p$  is the specific heat of tissue,  $C_b$  is the specific heat of blood,  $T$  is the temperature,  $q$  is the heat flux and  $q^r$  is the radiative heat flux.  $\omega_b$  is set to zero if there is no blood perfusion as is the case for tissue phantoms.

The radiative heat flux can be expressed in terms of temperature using previously calculated intensity distribution in the following way:

$$\nabla \cdot q^r(r, z, t) = k_a \left( 4n^2 \sigma_s T^4 - \int_{4\pi} \Phi(\Omega, \Omega) I(r, z, \Omega, t) d\Omega \right) \quad (6)$$

where  $n$  is refractive index of tissue medium and  $\sigma_s$  is Stephan-Boltzmann constant.

Heat flux due to conduction within the tissue medium can be expressed in terms of temperature distribution using either Fourier or non-Fourier heat conduction model. Heat conduction considering Fourier heat conduction model is expressed by following equation:

$$q(r, z, t) = -\kappa \nabla T(r, z, t) \quad (7)$$

where  $\kappa$  is the thermal conductivity of tissue and  $\nabla$  is the gradient.

The above parabolic diffusion equation implies an infinite speed of propagation of the thermal wave through the tissue medium. To eliminate this assumption of infinite speed of propagation of the thermal signal, a non-Fourier damped wave heat conduction model that takes into account finite speed of propagation of heat wave is considered and is given by [25, 29-31]:

$$q(r, z, t) + \tau \frac{\partial q(r, z, t)}{\partial t} = -\kappa \nabla T(r, z, t) \quad (8)$$

where  $\tau$  is the relaxation time of the medium.

Eq. (5), (6), (7) or Eq. (5), (6), (8) are simultaneously solved using suitable numerical scheme to obtain final temperature distribution as predicted by Fourier or non-Fourier heat conduction model respectively.

The boundary conditions that are used are the following: (i) all the boundaries except the top laser incident surface are insulated, (ii) at the top surface convective heat exchange (convective heat transfer coefficient = 10 W /m<sup>2</sup>.K)

with surrounding ambient air (25°C) is considered, (iii) the temperature profile is symmetric about the z-axis, and (iv) initially ( $t = 0$ ) the temperature is equal to the ambient temperature and its derivative with respect time are zero everywhere in space. In the present tissue phantom model, the following simplifications are introduced: (1) radiation emission from the tissue phantom is neglected because the tissue blackbody intensity is much smaller than the incident laser intensity; (2) tissue optical and thermal properties are thermally stable during the heat transfer process; (3) blood perfusion and thermal evaporation and/or phase change of tissue during the heat transfer process are not considered.

#### Solution scheme

The TDOM with  $S_{10}$  scheme is employed for the solution of the transient radiation transfer equations. For information on the numerical scheme and accuracy validation, please refer to the recent publication of the authors [28]. Therefore, the details of the numerical method on radiative transfer are not repeated here.

To solve the hyperbolic heat conduction equations, MacCormack's predictor-corrector scheme is adopted. The details of this method are presented in reference [32].

#### EXPERIMENTAL METHODS

The schematic of the experimental set up is shown in Fig. 2. A Q-switched short pulse Nd:YAG laser operating at a wavelength of 1064 nm and having a temporal pulse width ( $t_p$ ) of 200 ns (FWHM) is used in this study. During the experiment the laser power is constantly monitored using a power meter. The samples are well insulated on all sides (except on the irradiated face) to prevent heat loss to the surroundings. A thermal imaging camera (IR Flexcam Pro, Infrared Solutions) is used to record the radial surface temperature profile of the samples. The images are recorded with computerized data acquisition system and processed with National Instruments IMAQ Vision Builder Image processing software. The camera provides a measurement range of 0°C to 350°C with a sensitivity of  $\pm 0.09^\circ\text{C}$  at 30°C. The spectral response of the camera is 8 to 14  $\mu\text{m}$ . For the axial temperature measurements in the tissue phantom, holes are drilled up to the central axis at discrete locations along the length of the phantom (see Fig. 1). T-type thermocouples having diameter of 0.5 mm are inserted into the holes for temperature measurements. Temperature readings of the thermocouples are recorded through a computerized data acquisition system using Labview Software. These thermocouples provide a measurement range from 0°C to 480°C with a sensitivity of  $\pm 1^\circ\text{C}$  and 0.2 seconds of response time.

Experiments are performed on both single-layer and three-layer tissue phantoms replicating skin layers and having an embedded inhomogeneity simulating tumors (Fig. 1). The phantoms are composed of araldite, DDSA (Dodecenyl Succinic Anhydride) resin and DMP-30 (hardener) mixed in the ratio 1:0.87:0.04. Titanium Dioxide particles (mean diameter = 0.3  $\mu\text{m}$ ) are added as scatterer to the sample. India ink is used as absorber. Details about phantom preparation can be found in the previous papers of the authors [33]. The layered tissue phantom consists of three-layers having different optical properties representing epidermis, dermis, and fatty tissues of

human skin. The thickness, absorption coefficient ( $k_a$ ), and scattering coefficient ( $k_s$ ) of each layer are tabulated in Table 1. For single-layer tissue phantom, the base tissue matrix has bulk average absorption coefficient ( $k_a$ ) = 0.051  $\text{mm}^{-1}$ , and scattering coefficient ( $k_s$ ) = 6.14  $\text{mm}^{-1}$ . These values are obtained by calculating weighted average of properties of different layers of layered tissue phantom. The density ( $\rho$ ) of the medium is 1000  $\text{kg/m}^3$ , thermal conductivity ( $\kappa$ ) is 0.35 W/m.K, and the specific heat ( $C_p$ ) is taken as 4200 J/kg.K for all layers of tissue medium [22]. Inhomogeneities are drilled in tissue phantoms having scattering coefficient of 12.28  $\text{mm}^{-1}$  and absorption coefficient of 0.051  $\text{mm}^{-1}$ .

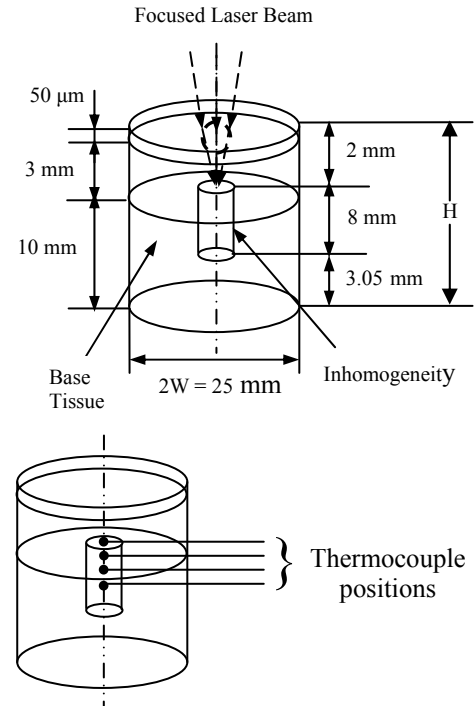


FIG. 1: SCHEMATIC OF TISSUE PHANTOM CONTAINING INHOMOGENEITY.

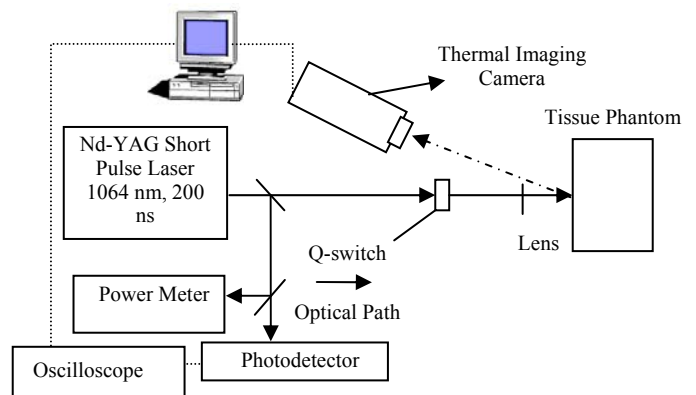


FIG. 2: SCHEMATIC OF THE EXPERIMENTAL SET-UP FOR TISSUE IRRADIATION USING SHORT PULSE LASER.

**TABLE 1: OPTICAL PROPERTIES OF DIFFERENT LAYERS OF HUMAN SKIN TISSUE AT 1064 NM [34, 35].**

Layer	Thickness (mm)	Absorption Coefficient ( $k_a$ ) ( $\text{mm}^{-1}$ )	Scattering Coefficient ( $k_s$ ) ( $\text{mm}^{-1}$ )
Epidermis	0.05	0.355	8.237
Dermis	3	0.049	8.237
Fatty tissue	10	0.050	5.5

## RESULTS AND DISCUSSION

In this paper temperature distribution in tissue medium during short pulse laser irradiation has been obtained both experimentally and using numerical model. Radial and axial temperature distributions are obtained for the case of three-layer and single-layer tissue phantoms for the case of both collimated and focused laser beam. Numerical modeling results are obtained for both hyperbolic non-Fourier and parabolic Fourier case by solving a coupled set of equations consisting of the transient radiative transport equation and Pennes' bio-heat transfer equation.

Experiments are performed on a three-layer tissue phantom containing inhomogeneity using focused laser beam. The embedded inhomogeneity simulating tumor is drilled 2 mm underneath the phantom surface. For the case of focused laser beam, the laser is focused directly at the inhomogeneity location ( $z = 2$  mm) using a converging lens. It has already been discussed earlier that a temperature rise of approximately  $43^\circ\text{C}$  is required for successfully irradiating tumors. Therefore, the sample is irradiated until  $43^\circ\text{C}$  temperature rise is obtained at the focal plane, which is at the inhomogeneity location. The surface temperature is measured using thermal camera and the temperature at  $z = 2$  mm is measured using thermocouples.

It has been observed that the accuracy of prediction provided by hyperbolic heat conduction model depends on proper choice of thermal relaxation time ( $\tau$ ). The value of  $\tau$  depends on the propagation velocity of thermal wave which is dependent on material structure and property. Although its value has been measured for biological media such as bologna meat samples [20], the exact value of thermal relaxation time (typically having values in the range of 10 to 20 seconds) is unknown for most of the tissues. Fig. 3a shows radial temperature distribution at the inhomogeneity location respectively for the case of three-layer tissue phantom for different relaxation times (ranging from 10 seconds to 20 seconds). The results obtained using Fourier heat conduction model is also plotted. These numerically predicted results are compared with corresponding experimentally measured temperature distributions. The error bars are plotted in the Fig. 3a represent uncertainty in experimental measurements. Considering a 99% confidence interval, the precision index for a total of three runs is calculated. The standard deviation between the three runs at each individual nodal point is evaluated. Thus the total uncertainty values at each nodal point is the product of the precision index times the standard deviation. It is observed that a maximum total uncertainty of  $1.515^\circ\text{C}$  is obtained for thermal camera and  $1.175^\circ\text{C}$  for thermocouple. It is clear from Fig. 3a that for human skin tissue

phantom, non-Fourier heat conduction model matches better with the experimental measurements for  $\tau = 15$  seconds. Fourier model predicts a significant lower temperature rise at the surface. Location of thermocouple at different radial locations may not be accurate and hence some deviation between experimental measurements and hyperbolic model is observed particularly for locations away from the laser beam axis. Corresponding axial temperature distribution plotted in Fig. 3b also shows that hyperbolic heat conduction model for  $\tau = 15$  seconds matches well with experimentally measured temperature distribution. This suggests that while studying heat transfer phenomena for a time scale shorter than the thermal relaxation time of the material,  $\tau$  is one of the governing parameter. Without considering proper value of  $\tau$ , bio-heat transfer models involving such analysis will produce erroneous temperature distributions. Therefore, for the case of tissue phantoms the value of  $\tau$  is taken as 15 seconds.

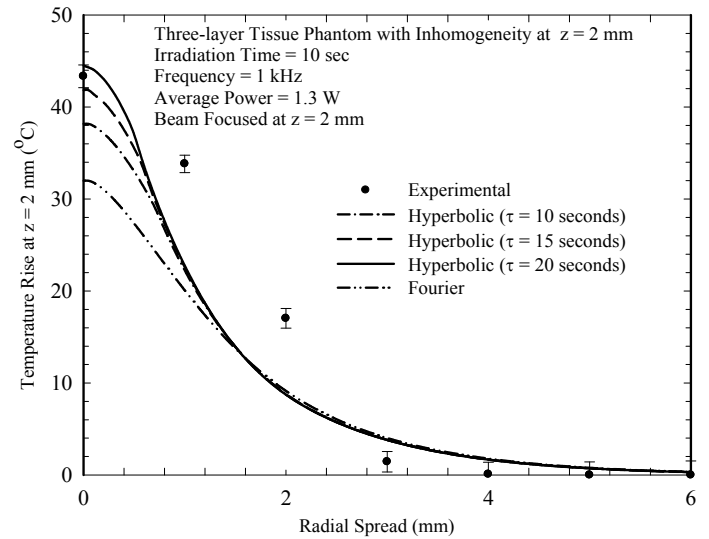


**FIG. 3A: RADIAL TEMPERATURE DISTRIBUTION AT THE INHOMOGENEITY LOCATION IN A THREE-LAYER TISSUE PHANTOM FOR DIFFERENT RELAXATION TIMES.**

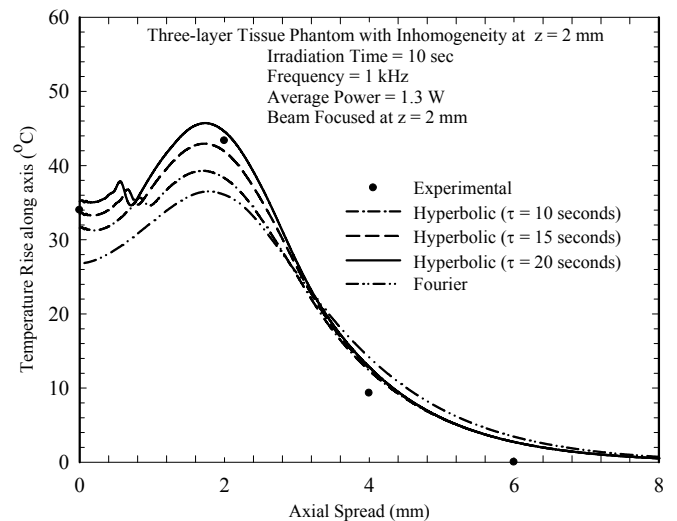


**FIG. 3B: AXIAL TEMPERATURE DISTRIBUTION IN A THREE-LAYER TISSUE PHANTOM FOR DIFFERENT RELAXATION TIMES.**

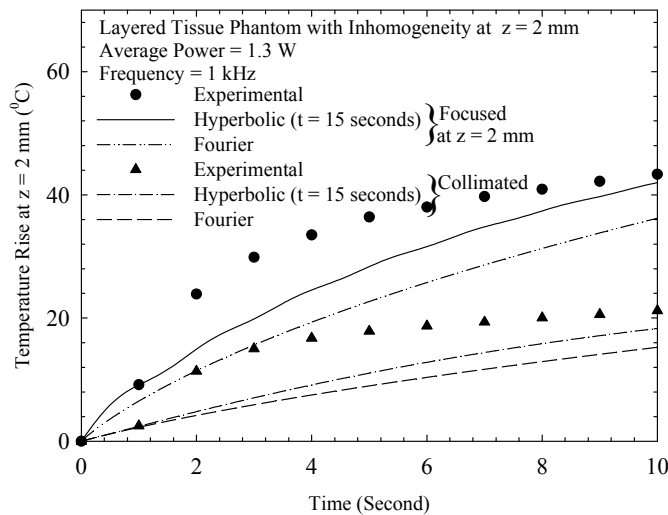


**FIG. 4A: COMPARISON OF TEMPERATURE HISTORY AT THE INHOMOGENEITY LOCATION BETWEEN COLLIMATED AND FOCUSED LASER BEAM IRRADIATION FOR A THREE-LAYER TISSUE PHANTOM.**

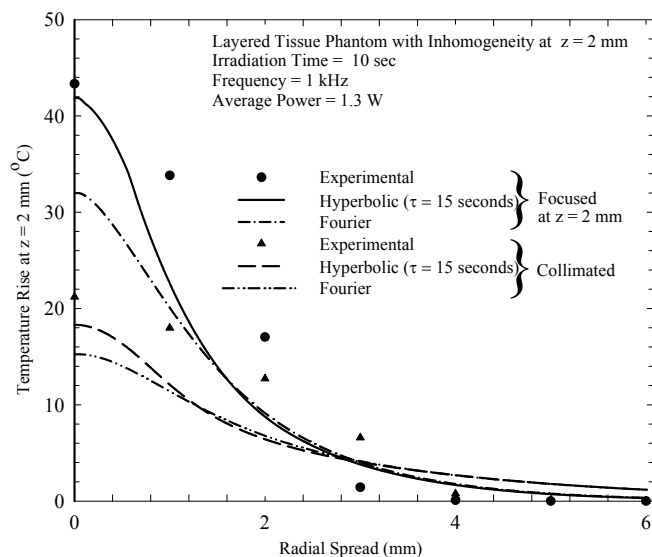
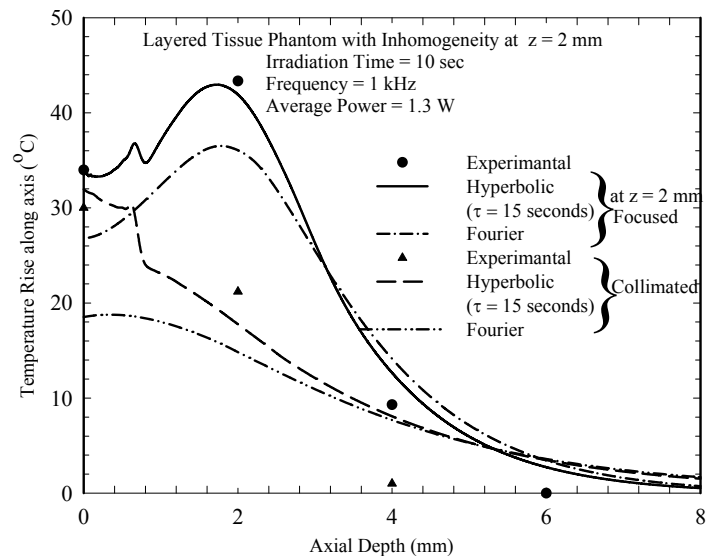


**FIG. 4B: COMPARISON OF RADIAL TEMPERATURE DISTRIBUTION AT THE INHOMOGENEITY LOCATION BETWEEN COLLIMATED AND FOCUSED LASER BEAM IRRADIATION FOR A THREE-LAYER TISSUE PHANTOM.**

Once selection of proper value of  $\tau$  for the numerical model is accomplished, experiments are performed to demonstrate the advantage of using focused laser beam for subsurface tumor irradiation. Fig 4a shows the temperature rise at the inhomogeneity location with time for the case of collimated and focused laser irradiation. The plot shows experimental data along with numerical modeling results obtained from hyperbolic heat conduction and Fourier heat conduction model. It is observed that converging laser beam focused at subsurface location can produce much higher temperature at that desired location as compared to collimated laser beam which is necessary for subsurface tumor irradiation. The deviation of experimental data from numerical modeling results is due to the



**DISTRIBUTION BETWEEN COLLIMATED AND FOCUSED LASER BEAM IRRADIATION FOR A THREE-LAYER TISSUE PHANTOM CONTAINING INHOMOGENEITY.**

limitation of placing the thermocouple at the exact location. Fig. 4b shows comparison of radial temperature distribution between experimental measurements and numerical modeling results obtained at inhomogeneity location (at  $z = 2$  mm) for collimated and focused laser irradiation after 10 seconds of laser exposure. Corresponding axial temperature distribution is plotted in Fig 4c. In this figure temperature distribution obtained from hyperbolic heat conduction model shows a wave phenomenon. Experimental measurements could not capture this effect due to the limitation of placing thermocouples very close to each other (currently there is a separation distance of 2 mm between two consecutive thermocouples).

After demonstrating the advantage of using focused laser beam and performing model validation studies in layered tissue phantom, experiments are conducted to compare the temperature distribution between a single-layer and three-layer tissue phantom. Conventionally, skin is treated as a single-layer medium for simplicity. But in reality, skin is a multi-layered medium having different thicknesses, scattering, and absorption coefficients in each layer (see Table 1). The goal of this part of the work is to investigate whether single-layer approximation of layered skin tissue is reasonable approximation or not. The radial temperature distribution at the inhomogeneity location ( $z = 2$  mm) for the case of a single-layer tissue phantom is compared with that of a three-layer tissue phantom in Fig. 5a. It is evident from figure that for the case of three-layer tissue phantom, the peak temperature rise is less but the radial heat spread is slightly more as compared to those of single-layer tissue phantom. These differences can be attributed to the consideration of average optical properties throughout the whole tissue phantom in case of single-layer model. Also, axial temperature distribution (Fig. 5b) obtained from thermocouples placed at various depths of the phantom shows lower peak temperature rise (obtained at  $z = 2$  mm) and smaller axial heat spread for three-layer tissue phantom. This is due to greater attenuation of laser beam caused by higher absorption coefficient of the first layer of three-layer tissue phantom as compared to single-layer tissue phantom. The top layer of the

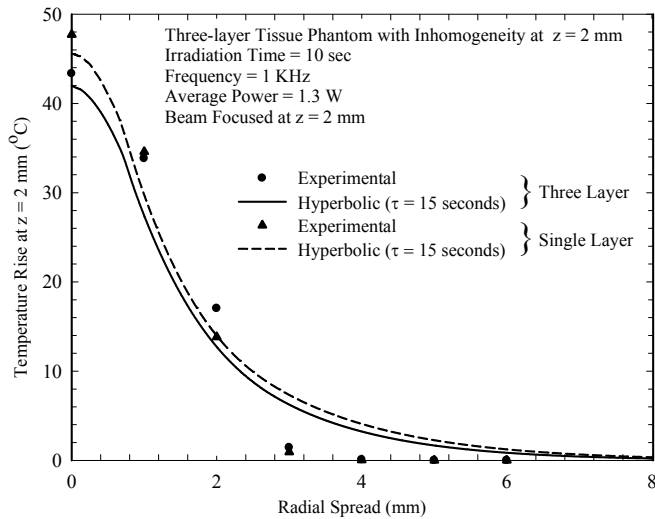


**FIG. 5A: COMPARISON OF RADIAL TEMPERATURE DISTRIBUTION AT THE INHOMOGENEITY LOCATION BETWEEN A SINGLE-LAYER AND A THREE-LAYER TISSUE PHANTOM FOR FOCUSED LASER BEAM IRRADIATION.**

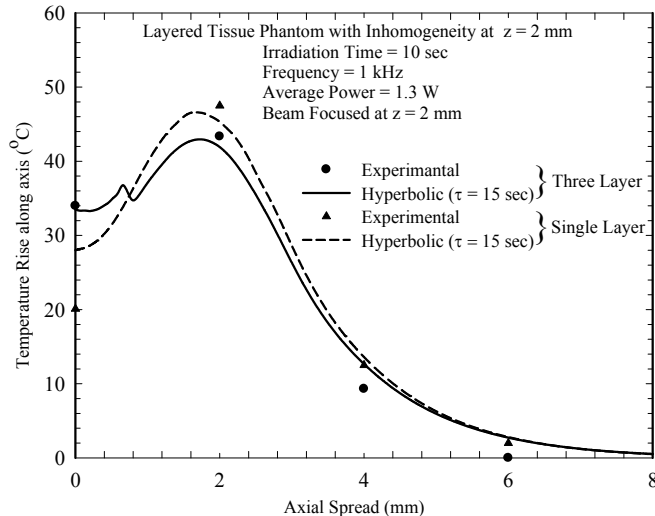


**FIG. 5B: COMPARISON OF AXIAL TEMPERATURE DISTRIBUTION BETWEEN A SINGLE-LAYER AND A THREE-LAYER TISSUE PHANTOM FOR FOCUSED LASER BEAM IRRADIATION.**

skin (epidermis) has high absorption coefficient which results in higher temperature rise at the surface in three-layer model than that of single-layer model. These results demonstrate that there is difference in heat affected zone in single-layer and three-layer model and hence skin should be modeled as a layered medium to analyze bio-heat transport phenomenon during short pulse laser irradiation of tissues.

## CONCLUSION

In this work skin tissue is modeled as a layered medium to analyze heat transfer during collimated and focused laser irradiation. This study demonstrates that converging laser beam focused at subsurface location can produce high

temperature rise at the desired subsurface location keeping the surface temperature low. The radial and axial temperature distributions obtained for multi-layer tissue phantoms during collimated and focused laser irradiation show that the focused beam can produce much compact heat affected zone as compared to that of collimated laser beam. It is demonstrated that the hyperbolic heat conduction model is an accurate model for such kind of analysis as it takes into account the relaxation time of the tissues. Fourier parabolic heat conduction model, on the other hand, is found to deviate significantly from experimental measurements. This analysis emphasizes importance of considering hyperbolic heat conduction formulation in studying heat transfer phenomenon for a time scale shorter than thermal relaxation time of the medium.

## ACKNOWLEDGMENTS

Kunal Mitra acknowledges partial support from Raydiance Inc. for this research.

## REFERENCES

- [1] Panjehpour M., Wilke A., Frazier D.L., Overholt B.F. 1991 "Hyperthermia treatment using a computer controlled Nd:YAG laser system in combination with surface cooling," *Proceedings of SPIE*, **1427**, pp. 307-315.
- [2] Manns F., Milne P.J., Gonzalez-Cirre X., Denham D.B., Parel J.M., Robinson D.S, 1998, "In-situ temperature measurements with thermocouple probes during laser interstitial thermometry (LITT): quantification and correction of a measurement artifact," *Lasers in Surgery and Medicine*, **23**, pp. 94-103.
- [3] Jeong S.W., Liu H., Chen W.R., 2003, "Temperature control in deep tumor treatment," *Proceedings of SPIE*, **5068**, pp. 216-216.
- [4] Wahrburg J., Schmidt K.U., 1997, "A new system for minimal invasive ablation of deep seated brain tumors," *Proceedings of IEEE/EMBS*, pp. 2438-2441.
- [5] Van Leeuwen T.G., Jansen E.D., Motamedi M., Borst C., Welch A.J, 1995, "Physics of Laser induced hyperthermia," In: *Welch AJ and van Germet MJC eds. Optical-thermal response of laser-irradiated tissue*, New York: Plenum, pp. 789-829.
- [6] Feyh J., Gutmann R., Leunig A., Jager L., Reiser M., Saxton R.E., Castro D.J., Kastenbauer M.D., "MRI-Guided laser interstitial thermal therapy (LITT) of head and neck tumors: progress with a new method," *Journal of Clinical Laser Medicine and Surgery*, **14**, pp. 361-366.
- [7] Sapareto S.A., Dewey W.C., 1984, "Thermal dose determination in cancer therapy," *International Journal of Radiation Oncology Biology Physics*, **10**, pp. 787-800.
- [8] Arora, D., Skliar, M., Roemer, R.B., 2005, "Minimum-time thermal dose control of thermal therapies," *IEEE Transactions on Biomedical Engineering*, **52**, pp. 191-200.
- [9] Robinson D.S., Parel J.M., Denham D.B., Gonzalez-Cirre X., Manns F., Milne P.J., Schachner R.D., Herron A.J., Comander J., Hauptmann G, 1998, "Interstitial laser hyperthermia model development for minimally invasive therapy of breast carcinoma," *Journal of American College of Surgeons*, **186**, pp. 284-292.

- [10] Zangos S., Mark M.G., Balzer J.O., Engelmann B.K., Straub R., Eichler K., Hergoz C., Lehnert T., Sollner O., Heller M., Thalhammer A., Vogl T.J., 2004, "Neoadjuvant transarterial chemoembolization (TACE) before percutaneous MR-guided laser-induced thermotherapy (LITT): Results in large-size primary and secondary liver tumors," *Medical Laser Application*, **19**, pp. 98-108.
- [11] Pech M., Wieners G., Fischbach F., Hengst S., Beck A., Warschewske G., Hanninen E.L., Wust P., Ricke J., 2004, "Synchronous CT-guided brachytherapy in patients at risk for incomplete interstitial laser ablation of liver malignancies," *Medical Laser Application*, **19**, pp. 73-82.
- [12] van Gemert M.J.C., Welch A.J. 1989, "Clinical use of laser-tissue interaction," *IEEE Engineering in Medicine and Biology Magazine*, pp. 10-13.
- [13] Wang L., Liang X., Galland P.A., Ho P.P., Alfano R.R. 1999, "Detection of objects hidden in highly scattering media using time-gated imaging methods," *Proceedings of SPIE*, **4082**, pp. 261-264.
- [14] Manstein D., Herron G.S., Sink R.K., Tanner H., Anderson R.R. 2004, "Fractional photothermolysis: a new concept for cutaneous remodeling using microscopic patterns thermal injury," *Lasers in Surgery and Medicine*, **34**, pp. 426-438.
- [15] Khan, M.H., Sink, R.K., Manstein, D., Eimerl, D., Anderson, R.R., 2005, "Intradermally focused infrared laser pulses: thermal effects at defined tissue depths," *Lasers in Surgery and Medicine*, **36**, pp. 270-280.
- [16] Gratzl T., Dohr G., Schmidt-Kloiber H., Reichel E., 1991, "Histological distinction of mechanical and thermal defects produced by nanosecond laser pulses in striated muscle at 1064 nm," *Proceedings of SPIE*, **1427**, pp. 55-62.
- [17] Joseph D.D., Preziosi L., 1989, *Heat Waves. Reviews of Modern Physics*, **61**, pp. 41-73.
- [18] Antaki, P.J., 2005, "New interpretation of non-Fourier heat conduction in processed meat," *ASME Journal Heat Transfer*, **127**, pp. 189-193.
- [19] Kaminski, W., 1990, "Hyperbolic heat conduction equation for materials with a nonhomogenous inner structure," *ASME Journal Heat Transfer*, **112**, pp. 555-560.
- [20] Mitra, K., Kumar S., Vedavarz, A., Moallemi, M.K., 1995, "Experimental evidence of hyperbolic heat conduction in processed meat," *ASME Journal of Heat Transfer*, **117**, pp. 568-573.
- [21] Chen W.R., 2003, "Selective photothermal interaction using near-infrared laser and laser absorbing dye in gel phantom and chicken breast tissue," *Proceedings of SPIE*, **4617**, pp. 18-25.
- [22] Liu, J., Chen, X., Xu, L.X., 1999, "New thermal wave aspects on burn evaluation of skin subjected to instantaneous heating," *IEEE Transactions on Biomedical Engineering*, **46**, pp. 420-428.
- [23] Deng Z.S., Liu J., 2002, "Analytical study on bioheat transfer problems with spatial or transient heating on skin surface or inside biological bodies," *Journal of Biomechanical Engineering - ASME*, **124**, pp. 638-649.
- [24] Huillier J.P.L., 1997, "Theoretical Analysis of the Role Played by Tissue-Optical Parameters in Laser Ablation Process," *Proceedings of SPIE*, **3195**, pp. 151-165.
- [25] Banerjee A., Ogale A., Das C., Mitra K., Subramanian C., 2005, "Temperature distribution in different materials due to short pulse laser irradiation" *Journal of Heat Transfer Engineering*, **26**, pp. 41-49.
- [26] Guo Z., Wan S.K., Kim K.H., and Kosaraju C., 2003, "Comparing diffusion approximation with radiation transfer analysis for light transport in tissues", *Opt. Rev.*, **10**, 415-421.
- [27] Modest M. F. 2003, *Radiative Heat Transfer*, Second Edition, McGraw-Hill, New York.
- [28] Kim K.H. and Guo Z., 2004, "Ultrafast radiation heat transfer in laser tissue welding and soldering", *Numerical Heat Transfer A*, **46**, 23-46.
- [29] Ozisik, M.N., Tzou, D.Y., 1994, "On the wave theory of heat conduction," *ASME Journal of Heat Transfer*, **116**, 526-535.
- [30] Kaminski, W., 1990, "Hyperbolic heat conduction equation for materials with a nonhomogenous inner structure," *ASME Journal Heat Transfer*, **112**, pp. 555-560.
- [31] Vedavarz, A., Mitra, K., Kumar S., 1994, "Hyperbolic temperature profiles for laser surface interactions," *Journal of Applied Physics*, **76**, pp. 5014-5021.
- [32] Kim K.H. and Guo Z., 2007, "Multi-time-scale heat transfer modeling of turbid tissues exposed to short-pulsed irradiations", *Computer Methods and Programs in Biomedicine*, **86**, 112-123.
- [33] Das, C., Trivedi, A., Mitra, K., Vo-Dinh, T., 2003, "Experimental and numerical analysis of short pulse laser interaction with tissue phantoms containing inhomogeneities," *Applied Optics*, **42**, pp. 5173-5180.
- [34] Djorev, P.L., Borisova, E., Avramov, L., 2003, "Interaction of the IR laser radiation with human skin - Monte-Carlo simulation," *Proceedings of SPIE - The International Society for Optical Engineering*, **5226**, pp. 403-407.
- [35] Simpson, R.C., Kohl, M., Essenpreis, M., Cope, M., 1998, "Near-infrared optical properties of ex vivo human skin and subcutaneous tissues measured using the Monte Carlo inversion technique," *Physics in Medicine and Biology*, **43**, pp. 2465-2478.